Lasers in Medical Science (2019) 34:1503–1508
https://doi.org/10.1007/s10103-018-2595-5

BRIEF REPORT

Texture feature extraction of gray-level co-occurrence matrix for metastatic cancer cells using scanned laser pico-projection images

Meng-Jia Lian[1] · Chih-Ling Huang[2]

Received: 17 April 2018 / Accepted: 17 July 2018 / Published online: 24 July 2018

Abstract

Metastasis is responsible for 90% of all cancer-related deaths in humans, and the development of a rapid and promising solution for an early diagnosis of metastasis is required. The present study proposed a promising method combined with scanned laser pico-projection technique and typical texture feature (i.e., contrast, correlation, energy, entropy, and homogeneity) extraction of gray-level co-occurrence matrix (GLCM) image processing model to classify the low- and high-metastatic cancer cells using five common cancer adenocarcinoma cell line pairs (i.e., HeLa/HeLa-S3, CL1-0/CL1-5, OVTW59-P0/OVTW59-P4, and CE81T-FN^{low}/CE81T-FN^{high} cell lines). Highly metastatic cancer cells essentially have the highest levels of disorder. Both contrast and entropy refer to the degree of disorder, and energy and homogeneity refer to the degree of uniformity. These four texture features can be effective evaluation indexes for disorder in cancer cells responding to metastatic ability. Texture feature extraction forms reflection images, which are recorded with scanned laser pico-projection system; they effectively bridge the gap in information derived from transmission images. The low- and high-metastatic cancer cells are statistically and effectively classified from the texture feature of GLCM through transmission and reflection images taken with scanned laser pico-projection system. In particular, it only requires several seconds after producing a confluent monolayer of cells and achieves the rapid method with a more reliable diagnostic performance for metastatic ability of cancer cells in vitro or ex vivo.

Keywords Metastasis · Cancer cell · Gray-level co-occurrence matrix · Scanned laser pico-projection · Image analysis

Introduction

Metastasis is a cancer-aggravated situation and causes treatment failures for 90% of all cancer-related deaths [1]. Metastasis means that cancer cells break away from the primary tumor site, travel throughout the body via the bloodstream or the lymphatic system, and initiate new growths at distant sites [2]. In clinical cases, many medical imaging techniques have been used to diagnose metastatic cancers, including X-rays, computed tomography, positron emission tomography, ultrasonography, and magnetic resonance imaging [3]. However, these techniques can only capture the images of cancer which have already moved to the second region from the original site by metastasis. If metastasis has already occurred, such techniques are not effective in prevention by predicting the metastatic ability of the cancer. Metastasis is a complex process involving cell proliferation, motility, and invasion. Therefore, the estimation of cell migration is a traditional method to evaluate the metastatic tendency of cancer cells. Wound healing assay is a typical test for cell migration, which requires at least 24 h after producing a confluent monolayer of cells [4]. A rapid and promising solution for the early diagnosis of metastasis needs to be developed.

Gray-level co-occurrence matrix (GLCM) was used by D. Molina et al. [5] to analyze the medical imaging on brain tumor heterogeneity obtained from magnetic resonance imaging and find its potential relationship with tumor malignancy (H. Zhou et al. [6]), extracting radiomic data from CT images of patients with lung cancer. Features are extracted from within the defined tumor contours on the CT images, quantifying tumor intensity, shape, texture, and Gabor and wavelet texture. GLCM provides a general statistical method for texture recognition of images [7]; however, its basic limitation is that the associated information is derived from grayscale images.

✉ Chih-Ling Huang
chihling@kmu.edu.tw

[1] School of Dentistry, Kaohsiung Medical University, Kaohsiung 807, Taiwan

[2] Center for Fundamental Science, Kaohsiung Medical University, Kaohsiung 807, Taiwan

To improve the ability of recognition, scanned laser pico-projection (SLPP) system was proposed to enhance the image variance. In real clinical cases, there are some devices that are like this system, such as colposcopy [8]. It provides the view with green filter for the vascular pattern of the cervix. It absorbs the red color and makes the appearance of blood vessels black for clear viewing. In this study, we try to use a new light source system, SLPP, to provide a routine quality assurance for imaging. The SLPP system can decrease the light intensity with Gaussian distribution from central to the margin via the scanning laser pico-projection technique for wide screen. Moreover, the SLPP system is a commercial projection device for wide screen and enhances the usability for imaging. Chuang et al. [9] presented a method for two-dimensional nanoparticle concentration measuring via the images obtained by the SLPP system. The feasibility was demonstrated by measuring type I collagen concentrations in the range of 0.025–0.125%. It shows that the SLPP system has a higher throughput, a lower cost, a larger sample size, and a more reliable diagnostic performance.

Based on the methodology, the useful SLPP system and the GLCM imaging analysis method can be combined to provide the classified method with the superior diagnostic performance. In the previous study, we do the effort in the case of biopsy from the patients, such as characterization for oral cancer by pathological images. The SLPP system combined with the GLCM image analysis method can differentiate the normal and cancerous pathological sections. The discrimination of normal and cancerous tissues was dominated by the disorder caused by the unusual proliferation and division of the cell nuclei and chromosomes inside [10]. It works on both full field and specific tissues analysis. Compared to the existing methods, the proposed method approach has many advantages, including a lower cost, a larger sample size, and a more reliable diagnostic performance. In this study, we try to provide a highly promising solution for the pathologists/doctors based on the SLPP system combined with the GLCM image analysis method for the diagnosis of metastatic cancer cells.

Materials and methods

The optical image system used in this study comprised SLPP (MicroVision; Model: SHOWWX™; Image size: 150–2500 mm) and a microscope (OLYMPUS BX-53). In accordance with the findings of previous studies, the samples were illuminated using a green laser source (wavelength = 532 nm) to obtain the optimal image quality. In obtaining the transmission and reflection images of cells, the samples were illuminated using a halogen lamp and the SLPP system. The SLPP image system was sketched and shown in Fig. 1. The images were all captured using a charge coupled device (CCD) camera (Model: 1500M-T1-GE S/N 3797) with DVC View™

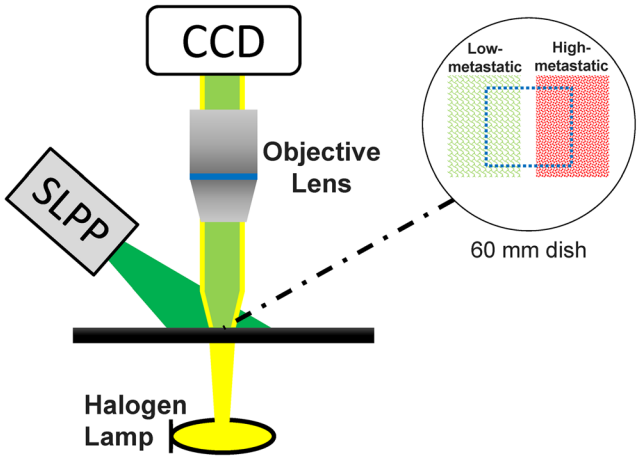

Fig. 1 The SLPP image system

image acquisition software with 1392 × 1040 pixels. Because the diameter of HeLa and HeLa-S3 cancer cell is approximately 10–20 pixels and the images with homogeneous cell distribution can be obtained with an image size of 150 × 150 pixels. Therefore, the images were separated into sub-images with a size of 150 × 150 pixels. Subsequently, the images with 256 gray-level images were processed by the GLCM model.

GLCM functions characterize the texture of images by calculating how often pairs of pixel with specific values and in a specific spatial relationship occur in an image, creating a GLCM, and then extracting statistical measures from this matrix [11]. Haralick et al. [12] defined the features by equations such that the texture feature of GLCM can be calculated including contrast, correlation, energy, entropy, and homogeneity. These five features are commonly involved in the investigation of biology. For example, the texture analyzer of the public domain, Java-based image processing program, *Image J*, developed at the National Institutes of Health also uses these five representative features.

The variable $C(i, j)$ expressed in Eqs. (5) refers to the value at the (i, j) position in a GLCM. These five features indicate the image texture, such as contrast indicates the presence of edges, noise, or wrinkled textures; correlation denotes the linear dependence on the neighboring pixels; energy represents the uniformity (or orderliness); entropy indicates the degree of disorder among pixels; and homogeneity represents the smoothness of the gray level distribution. In other words, these five texture features of GLCM correspond to the disorder in cell images, which indicate how the disorder is impacted by the metastatic ability of cancer cells.

$$\text{Contrast}: \sum_{ij=1}^{G} C_{ij}(i-j)^2 \tag{1}$$

$$\text{Correlation}: \sum_{ij=1}^{G} \frac{(i-u_i)(j-u_j)}{\sigma_i \sigma_j} C_{ij} \tag{2}$$

$$\text{Energy}: \sum_{ij=1}^{G} C_{ij}^{\,2} \tag{3}$$

$$\text{Entropy}: -\sum_{ij=1}^{G} C_{ij}\log C_{ij} \quad (4)$$

$$\text{Homogeneity}: \sum_{ij=1}^{G} \frac{1}{1+|i-j|} C_{ij} \quad (5)$$

In this study, we used HeLa/HeLa-S3 cancer cells, human cervical adenocarcinoma cell line, in order to evaluate the GLCM feature extraction model with the SLPP system, as HeLa cancer cell line is widely used for investigation in molecular biology [13] and biophysics [14]. Lung, ovarian, breast, and esophageal cancers are highly lethal; hence, the validity of the proposed method was demonstrated by using these five common cancer adenocarcinoma cell line pairs (i.e., HeLa/HeLa-S3, CL1-0/CL1-5, OVTW59-P0/OVTW59-P4, and CE81T-FN^{low}/CE81T-FN^{high} cell lines). All cells were maintained in a Dulbecco's Modified Eagle's Medium solution containing 10% fetal calf serum and incubated at 37 °C with 5% CO_2. The details of each cell line pair are described as follow.

HeLa/HeLa-S3: HeLa-S3 cells, which are high-metastatic cancer cells, are derivatives of the original HeLa cells and grow to a larger size in spherical colonies rather than as monolayers [15].

CL1-0/CL1-5: CL1-5 cells are highly invasive sublines compared to CL1-0 cells from the clonal cell line of human lung adenocarcinoma [16].

OVTW59-P0/OVTW59-P4: OVTW59-P4 are highly invasive sublines selected from epithelial ovarian OVTW59-P0 cells [17].

67NR/4T1: 67NR and 4T1 are low- and high-metastatic mouse mammary adenocarcinoma cell lines, respectively [18].

CE81T-Fn^{low}/CE81T-Fn^{high}: CE81T-Fn^{low} and CE81T-Fn^{high} are potentially low- and high-metastatic esophageal squamous carcinoma cell lines [19].

To evaluate the reliability of the detection method, the statistical differences between the low- and high-metastatic cells from the same origin, were evaluated using a one-way analysis of variance (ANOVA) technique. In evaluating the test results, a $*p$ value of < 0.05 was statistically significant, a $**p$ value of < 0.01 was very statistically significant, and a $***p$ value of < 0.001 was highly statistically significant.

Results and discussion

Texture feature extraction with GLCM extraction of various orientation angles and interpixel distances from transmission and reflection images of HeLa/HeLa-S3 metastatic cancer cell pairs is shown in Fig. 2. Fig. 2a–e shows the contrast, correlation, energy, entropy, and homogeneity extraction with an orientation angle of 0–270° with an interpixel distance of 10 pixels on x-axis. It shows that the values of these texture features are stable with various orientation angle increments, except correlation. In Fig. 2b, it shows the correlation and the correlation denotes the linear dependence on the neighboring pixels. But, we can see the random distribution of cells and the shapes of the cells are not entirely similar, which affects the correlation extraction at various orientation angles. The difference of correlation values is caused by the random distribution and cell shape but not correspond to the angular dependence. Especially, the value of correlation is much lower (e.g., the order of $10^{\wedge-4}$). However, extraction of the rest of the texture feature (contrast, energy, entropy, and homogeneity) is reliable even when the orientation angle changes. In other words, we can set-up the specific value of the orientation angle (e.g., 0°) to obtain the typical texture features (contrast, energy, entropy, and homogeneity). Fig. 2f–j shows the contrast, correlation, energy, entropy, and homogeneity extraction with an interpixel distance of 0–150 pixels. The inflection points of texture feature can be found in Fig. 2f–j around an interpixel distance of 10–20 pixels. The size of the image used for processing is 150 × 150 pixels and the diameter of HeLa and HeLa-S3 cancer cell is approximately 10–20 pixels, which implies that the characteristic texture feature commonly occurs in the boundary of cells, and that we can set-up the specific value of interpixel distance (e.g., 10 pixels) around the cell diameter to obtain the typical texture features.

We can establish two important points from this analysis. First, HeLa-S3 cancer cells (high-metastatic) have higher contrast and entropy but lower energy and homogeneity. Both contrast and entropy refer to the degree of disorder, and energy and homogeneity refer to the degree of uniformity. These four texture features can be the effective evaluation indexes for disorder in cancer cells. Secondly, the disorder of cancer cells with metastatic ability can be exactly evaluated in combination with transmission and reflection images recorded by the SLPP system.

Transmission and reflection images of HeLa/HeLa-S3, CL1-0/CL1-5, OVTW59-P0/P4, 67NR/4T1, and CE81T-Fn^{low}/Fn^{high} metastatic cancer cell pairs are shown in Fig. 3. In Fig. 3a, most of the high-metastatic cancer cells have dense cytoplasm and display clear contrast in transmission images, except CL1-5. The high-metastatic CL1-5 cancer cells have a small and more three-dimensional shape, and it is difficult to observe the cytoplasm in the same focus plane, compared to CL1-0 cancer cells. The CL1-0/CL1-5 cancer cell pair is not easily classified using only transmission images. However, reflection images taken by SLPP system bring more information from cell surface contour. In Fig. 3b, the clear contrast was displayed in the reflection images of high-metastatic cancer cells. Combination with transmission and reflection images taken by SLPP system helps us classify the cancer cells with high-metastatic ability more evidently.

The texture feature of GLCM for transmission and reflection images of metastatic cancer cell pairs is shown in Table 1.

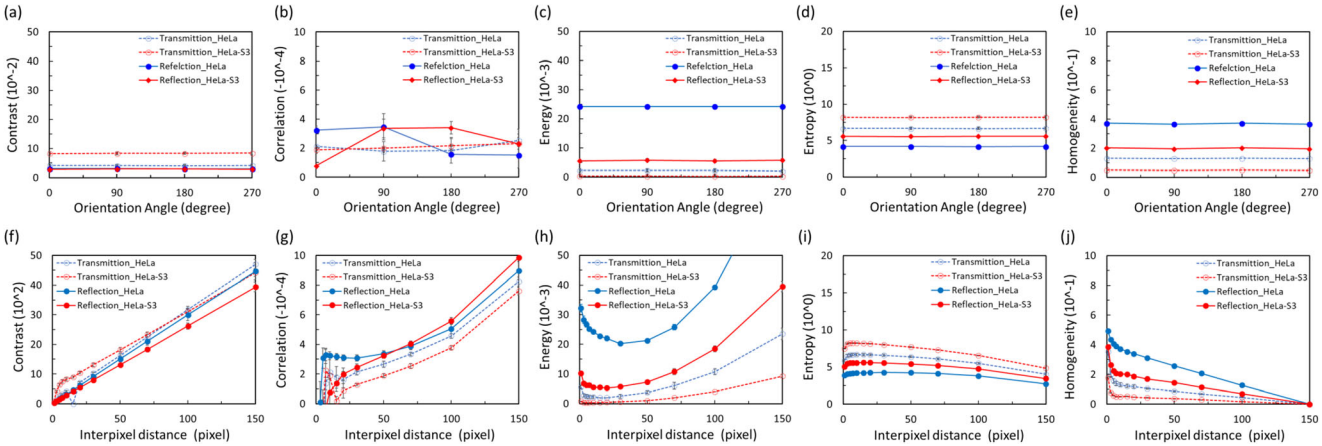

Fig. 2 Texture feature of GLCM for (**a**) contrast, (**b**) correlation, (**c**) energy, (**d**) entropy, and (**e**) homogeneity extraction with an orientation angle of 0–270° of HeLa/HeLa-S3 cancer cells. Panels (**f**)–(**j**) show texture feature of GLCM extraction with interpixel distance of 0–150 pixels of HeLa/HeLa-S3 cancer cells

The texture features of low-metastatic cancer cells are used as the benchmark and statistically compared with those of the high-metastatic cancer cells. High-metastatic cancer cells essentially exhibit high disorders, which makes the high-metastatic cancer cells display higher contrast and entropy, but lower energy and homogeneity. In HeLa/HeLa-3, CL1-0/CL1-5, and 67NR/4T1 cancer cell pairs, the texture feature of transmission images and reflection images taken by the SLPP system is successfully classified in low and high pairs. Especially in OVTW59-P0/P4 and CE81T-Fn^{low}/Fn^{high} cancer cell pairs, they are very difficult to classify via transmission images.

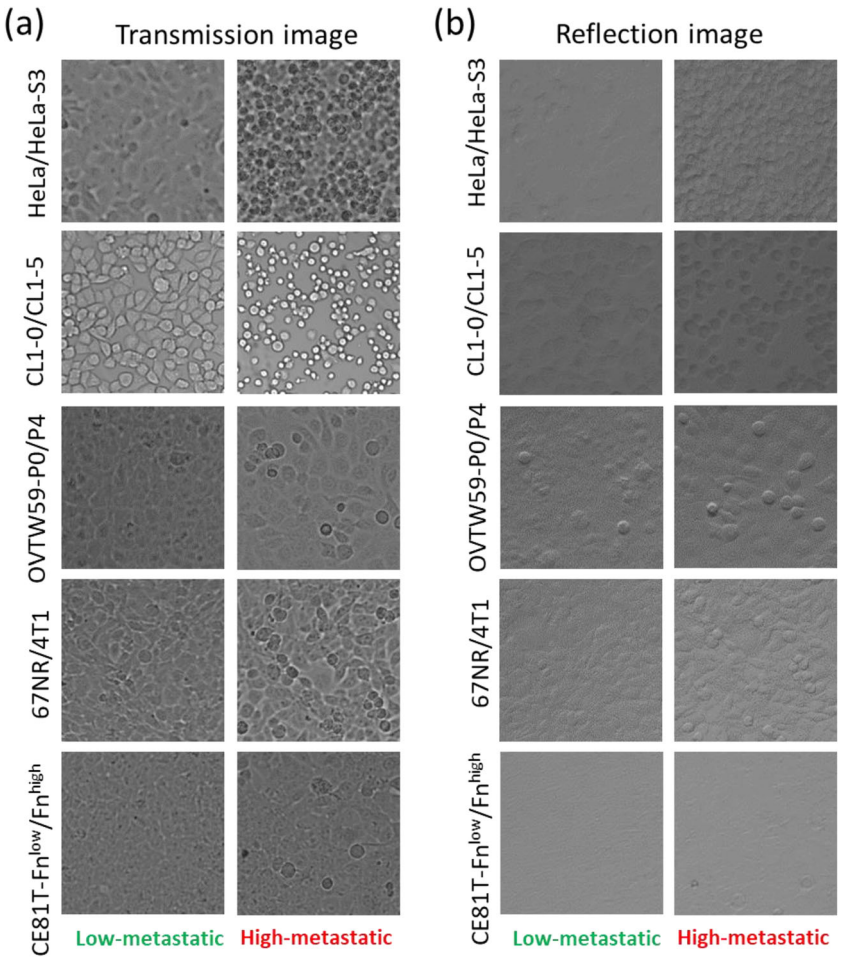

Fig. 3 **a** Transmission and (**b**) reflection images of HeLa/HeLa-S3, CL1-0/CL1-5, OVTW59-P0/P4, 67NR/4T1, and CE81T-Fn^{low}/Fn^{high} metastatic cancer cell pairs

Table 1 Texture feature of GLCM for transmission (*T.*) and reflection (*R.*) images of metastatic cancer cell pairs

Image type	Cell pair	Contrast (10^2)		Energy (10^−4)		Entropy (10^0)		Homogeneity (10^−1)	
T.	HeLa	4.2 ± 0.26	***	2.3 ± 5.0	***	6.7 ± 0.15	***	13.0 ± 1.2	***
	HeLa-S3	8.2 ± 0.51		3.6 ± 0.2		8.2 ± 0.06		5.0 ± 0.3	
	CL1-0	41.0 ± 2.60	***	2.4 ± 0.2	*	8.7 ± 0.10	$p = 0.59$	4.3 ± 0.5	*
	CL1-5	23.0 ± 1.80		6.1 ± 0.3		8.6 ± 0.28		7.4 ± 1.7	
	OVTW59-P0	3.5 ± 0.14	**	38.0 ± 9.6	$p = 0.09$	6.0 ± 0.22	$p = 0.68$	19.0 ± 0.9	$p = 0.13$
	OVTW59-P4	2.8 ± 0.27		50.0 ± 8.2		6.0 ± 0.22		17.0 ± 1.7	
	67NR	9.5 ± 2.10	*	4.0 ± 0.3	*	7.7 ± 0.23	**	7.3 ± 1.0	*
	4T1	13.0 ± 1.30		6.8 ± 1.7		8.2 ± 0.08		5.7 ± 0.3	
	CE81T-Fn^{low}	7.0 ± 0.59	$p = 0.14$	12.0 ± 5.2	$p = 0.93$	7.1 ± 0.29	$p = 0.52$	9.8 ± 1.5	$p = 0.33$
	CE81T-Fn^{high}	6.5 ± 0.30		13.0 ± 5.2		7.0 ± 0.08		11.0 ± 0.3	
R.	HeLa	3.1 ± 0.20	$p = 0.05$	24.0 ± 0.5	***	4.2 ± 0.03	***	3.7 ± 0.10	***
	HeLa-S3	2.8 ± 0.08		6.0 ± 0.6		5.6 ± 0.07		2.0 ± 0.07	
	CL1-0	4.6 ± 0.26	$p = 0.17$	12.0 ± 1.3	*	4.9 ± 0.11	**	2.9 ± 0.17	**
	CL1-5	4.3 ± 0.28		9.0 ± 1.0		5.3 ± 0.07		2.6 ± 0.11	
	OVTW59-P0	1.1 ± 0.35	$p = 0.53$	19.0 ± 3.4	$p = 0.17$	4.4 ± 0.19	*	3.8 ± 0.26	$p = 0.12$
	OVTW59-P4	1.3 ± 0.41		15.0 ± 3.0		4.8 ± 0.19		3.4 ± 2.60	
	67NR	1.4 ± 0.15	$p = 0.05$	14.0 ± 1.0	***	4.6 ± 0.09	***	3.1 ± 0.16	***
	4T1	1.9 ± 0.33		8.0 ± 1.3		5.3 ± 0.15		2.4 ± 1.50	
	CE81T-Fn^{low}	4.7 ± 0.20	$p = 0.47$	14.0 ± 0.0	*	4.6 ± 0.12	***	3.0 ± 0.04	$p = 0.17$
	CE81T-Fn^{high}	4.8 ± 0.16		12.0 ± 1.3		4.9 ± 0.11		2.9 ± 0.16	

Note: * represents $p < 0.05$, ** represents $p < 0.01$ and *** represents $p < 0.001$

First of all, the chosen cell lines were demonstrated that they are metastatic phenotypes according to the previous study. Second, the molecular profiles of the metastatic cells provide the evidence of protein and gene expression. However, metastasis is a complex process involving many stages, including homing, extravasations, micro-metastasis, co-opted stroma, and full colonization. Generally speaking, the high-metastatic cancer cells have a stronger proliferation ability and a large number of organelles within the cells. In addition, they have a stronger cell activity and a shorter cell cycle. The shorter time for mitosis preparation restricts the organelles formed and other biological molecules within it [20]. The mass and turbid matters render the transmission image with high disorder. Then, the high-metastatic cancer cells exhibit a spindle-like morphology and more three-dimensional structures with characteristic rough surfaces to increase cell migration and invasion [21]. These structures enhance the light scattering effect. The reflection images taken by the SLPP system exactly display the contour of the surface morphology, and reflection images of high-metastatic cancer cells also have high disorder. Conclusively, this system measured the equivalence of the metastatic phenotype according to the optical characteristic.

Texture feature extraction that forms reflection images taken by the SLPP system brings the effective information and supplies the information lacking in the transmission images. We can thus statistically and effectively classify the low- and high-metastatic pairs using the texture feature of GLCM, through transmission and reflection images taken by the SLPP system.

Conclusion

This technique can be applied in real clinical cases for tissues or biopsy from the patients wherein the images can just be taken from a camera. But it is not suitable for the cases in which images cannot be easily taken, such as ovarian cancer. However, the cancer cells can be extracted from ascites of patients and cell culture with mono-layered cells can resolve the problem for the image taken. Then, the method can be suitable for all cases for cancer cells. Transmission and reflection images taken by the SLPP system only require several seconds after producing a confluent monolayer of cells. In the present study, we proposed a promising method combined with the SLPP technique and the GLCM image processing model to achieve a rapid method with a more reliable diagnostic performance for metastatic ability of cancer cells in vitro or ex vivo.

Funding information The authors gratefully acknowledge the financial support provided for this study by the Ministry of Science and Technology (MOST) in Taiwan under Grant No. MOST-106-2221-E-037-004. This study is also supported by a grant from the Kaohsiung Medical University Research Foundation (KMU-Q107023).

Compliance with ethical standards

Conflict of interest The authors declare that they have no conflict of interest.

Ethical approval Approval by Ethical Commission is not needed.

Informed consent Not applicable since there are no patients involved.

References

1. Weigelt B, Peterse JL, van't Veer LJ (2005) Breast cancer metastasis: markers and models. Nat Rev Cancer 5:591–602
2. Stacker SA, Williams SP, Karnezis T, Shayan R, Fox SB, Achen MG (2014) Lymphangiogenesis and lymphatic vessel remodelling in cancer. *Nat Rev Cancer* 14:159–172
3. Kinkel K, Lu Y, Both M, Warren RS, Thoeni RF (2002) Detection of hepatic metastases from cancers of the gastrointestinal tract by using noninvasive imaging methods (US, CT, MR imaging, PET): a meta-analysis. Radiology 224:748–756
4. Wu Y, Liu ZG, Shi MQ, Yu HZ, Jiang XY, Yang AH et al (2017) Identification of ACTG2 functions as a promoter gene in hepatocellular carcinoma cells migration and tumor metastasis. Biochem Biophys Res Commun 491:537–544
5. Molina D, Pérez-Beteta J, Martínez-González A, Martino J, Velásquez C, Arana E et al (2016) Influence of gray level and space discretization on brain tumor heterogeneity measures obtained from magnetic resonance images. Comput Biol Med 78:49–57
6. Zhou H, Dong D, Chen B, Fang M, Cheng Y, Gan Y et al (2018) Diagnosis of distant metastasis of lung cancer: based on clinical and radiomic features. Transl Oncol 11:31–36
7. Hossain K, Parekh R (2010) Extending GLCM to include color information for texture recognition. AIP Conference Proceedings 1298:583–588
8. CT Lam, MS Krieger, JE Gallagher, B Asma, LC Muasher, JW Schmitt, et al., "Design of a novel low cost point of care tampon (POCkeT) colposcope for use in resource limited settings," PLoS ONE, vol. 10, p. e0135869, 09/02
9. Chuang CH, Sung TW, Huang CL, Lo YL (2012) Relative two-dimensional nanoparticle concentration measurement based on scanned laser pico-projection. Sensors Actuators B Chem 173: 281–287
10. M-J Lian, C-L Huang, and T.-M. Lee, "Automation characterization for oral cancer by pathological image processing with gray-level co-occurrence matrix," presented at the 5th International Conference on Mechanics and Mechatronics Research, Tokyo, 2018
11. Lloyd K, Rosin PL, Marshall D, Moore SC (May 01 2017) Detecting violent and abnormal crowd activity using temporal analysis of grey level co-occurrence matrix (GLCM)-based texture measures. Mach Vis Appl 28:361–371
12. R Haralick, K Shanmugam, and I H. Dinstein, Texture features for image classification vol. 3, 1975
13. Landry JJM, Pyl PT, Rausch T, Zichner T, Tekkedil MM, Stütz AM et al (2013) The genomic and transcriptomic landscape of a HeLa cell line. G3: Genes|Genomes|Genetics 3:1213–1224
14. Shiraga K, Suzuki T, Kondo N, Tanaka K, Ogawa Y (2015) Hydration state inside HeLa cell monolayer investigated with terahertz spectroscopy. Appl Phys Lett 106:253701
15. Puck TT, Marcus PI (1955) A rapid method for viable cell titration and clone production with HeLa cells in tissue culture: the use of X-irradiated cells to supply conditioning factors. Proc Natl Acad Sci U S A 41:432–437
16. Chu YW, Yang PC, Yang SC, Shyu YC, Hendrix MJ, Wu R et al (1997) Selection of invasive and metastatic subpopulations from a human lung adenocarcinoma cell line. Am J Respir Cell Mol Biol 17:353–360
17. Torng PL, Lee YC, Huang CY, Ye JH, Lin YS, Chu YW et al (2008) Insulin-like growth factor binding protein-3 (IGFBP-3) acts as an invasion-metastasis suppressor in ovarian endometrioid carcinoma. Oncogene 27:2137–2147
18. Aslakson CJ, Miller FR (1992) Selective events in the metastatic process defined by analysis of the sequential dissemination of subpopulations of a mouse mammary tumor. Cancer Res 52:1399–1405
19. Huang L, Cheng HC, Isom R, Chen CS, Levine RA, Pauli BU (2008) Protein kinase Cepsilon mediates polymeric fibronectin assembly on the surface of blood-borne rat breast cancer cells to promote pulmonary metastasis. J Biol Chem 283:7616–7627
20. Chan KS, Koh CG, Li HY (2012) Mitosis-targeted anti-cancer therapies: where they stand. Cell Death and Disease 3:e411
21. Diepenbruck M, Christofori G (2016) Epithelial–mesenchymal transition (EMT) and metastasis: yes, no, maybe? Curr Opin Cell Biol 43:7–13